MEMORANDUM REPORT BRL-MR-3792

# BRL

# COMPUTATIONAL FLUID DYNAMICS METHOD FOR LOW REYNOLDS NUMBER FLOW IN A PRECESSING/SPINNING, LIQUID-FILLED CYLINDER WITH ROUNDED ENDCAPS

MICHAEL J. NUSCA

DECEMBER 1989

U.S. ARMY LABORATORY COMMAND

## BALLISTIC RESEARCH LABORATORY
## ABERDEEN PROVING GROUND, MARYLAND

90 01 16 130

# DESTRUCTION NOTICE

## REPORT DOCUMENTATION PAGE

Form Approved
OMB No. 0704-0188

| 1a. REPORT SECURITY CLASSIFICATION UNCLASSIFIED | 1b. RESTRICTIVE MARKINGS |
|---|---|
| 2a. SECURITY CLASSIFICATION AUTHORITY | 3. DISTRIBUTION/AVAILABILITY OF REPORT Approved for public release; distribution is unlimited. |
| 2b. DECLASSIFICATION/DOWNGRADING SCHEDULE | |
| 4. PERFORMING ORGANIZATION REPORT NUMBER(S) BRL-MR-3792 | 5. MONITORING ORGANIZATION REPORT NUMBER(S) |

| 6a. NAME OF PERFORMING ORGANIZATION U.S. Army Ballistic Research Laboratory | 6b. OFFICE SYMBOL (If applicable) SLCBR-LF | 7a. NAME OF MONITORING ORGANIZATION |
|---|---|---|
| 6c. ADDRESS (City, State, and ZIP Code) Aberdeen Proving Ground, MD 21005-5066 | | 7b. ADDRESS (City, State, and ZIP Code) |

| 8a. NAME OF FUNDING/SPONSORING ORGANIZATION U.S. Army Ballistic Research Laboratory | 8b. OFFICE SYMBOL (If applicable) SLCBR-DD-T | 9. PROCUREMENT INSTRUMENT IDENTIFICATION NUMBER |
|---|---|---|

8c. ADDRESS (City, State, and ZIP Code)

Aberdeen Proving Ground, MD 21005-5066

10. SOURCE OF FUNDING NUMBERS

| PROGRAM ELEMENT NO. 62618A | PROJECT NO. 1L1 62618AH80 | TASK NO. | WORK UNIT ACCESSION NO. |
|---|---|---|---|

11. TITLE (Include Security Classification)

Computational Fluid Dynamics Method for Low Reynolds Number Flow in a Precessing/Spinning Liquid-Filled Cylinder with Rounded Endcaps (U)

12. PERSONAL AUTHOR(S)

Michael J. Nusca

| 13a. TYPE OF REPORT Memorandum Report | 13b. TIME COVERED FROM _____ TO _____ | 14. DATE OF REPORT (Year, Month, Day) | 15. PAGE COUNT 27 |
|---|---|---|---|

16. SUPPLEMENTARY NOTATION

17. COSATI CODES

| FIELD | GROUP | SUB-GROUP |
|---|---|---|
| 20 | 04 | |
| 19 | 01 | |

18. SUBJECT TERMS (Continue on reverse if necessary and identify by block number)

Finite Difference  Liquid Moment
Incompressible Flow  Low Reynolds Number
Liquid-Filled Projectile  Rotating Liquids

19. ABSTRACT (Continue on reverse if necessary and identify by block number)

The three-dimensional, steady, laminar, Navier-Stokes equations are solved using an implicit finite-difference scheme based on successive-over-relaxation. These numerical simulations are used to predict the behavior of incompressible liquids undergoing steady spin and steady precession at a fixed precession angle. The liquid is contained in a fully-filled cylinder with flat or rounded endcaps. These numerical simulations can predict steady viscous and pressure moments due to the liquid fill at low Reynolds number. These moments tend to increase the precession angle and reduce the spin rate of the container. Liquid-induced roll and side (yaw) moments are computed as functions of endcap height to cylinder radius ($0 < e/a < 1$), cylinder half-height to radius ($.5 < c/a < 4$), Reynolds number ($10 < Re < 300$), ratio of precession to spin rate ($.05 < \tau < .95$), and precession angle ($\alpha_c = 2°$). For a given cylinder, rounded endcaps can decrease the resonant liquid-induced moment by about 25% and shift the resonance to a smaller Reynolds number.

(Continued)

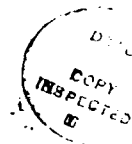| 20. DISTRIBUTION/AVAILABILITY OF ABSTRACT ☐ UNCLASSIFIED/UNLIMITED ☒ SAME AS RPT ☐ DTIC USERS | 21. ABSTRACT SECURITY CLASSIFICATION UNCLASSIFIED |
|---|---|
| 22a. NAME OF RESPONSIBLE INDIVIDUAL Michael J. Nusca | 22b. TELEPHONE (Include Area Code) (301)-278-2057  22c. OFFICE SYMBOL SLCBR-LF-A |

DD Form 1473, JUN 86  Previous editions are obsolete.

# Table of Contents

INTENTIONALLY LEFT BLANK.

# List of Figures

v

INTENTIONALLY LEFT BLANK.

# List of Tables

INTENTIONALLY LEFT BLANK.

# I. INTRODUCTION

The flight stability of liquid-filled, spin-stabilized projectiles has been considered for a wide variety of conditions, Originally, theories and experiments were centered about the case of large Reynolds number (Re = $a^2\phi/\nu$, see List of Symbols) for cylindrical payload containers.[1,2] Non-steady effects must be considered for practical applications and large Reynolds number, for example, spin-up.[3,4,5] However, if the Reynolds number is small (Re < 500), the effects of unsteady processes may be neglected. It is then possible to employ a steady finite-difference solution to the incompressible Navier-Stokes equations for a fixed precession angle and steady rates of spin and precession. Pressures have been measured under these conditions and can be used to validate numerical simulations.[6,7]

This report describes the steady-state finite-difference method of Strikwerda[8] that has been extensively investigated by Nusca[9] for fluid-filled cylindrical containers, and the extension of this code to non-cylindrical axisymmetric geometries. In particular, the case of a cylinder with rounded endcaps (see Figure 1) is investigated.

# II. BACKGROUND

In this section a steady-state computational fluid dynamics (CFD) method and an analytical simulation for cylindrical containers, are reviewed. Analytical and experimental work for non-cylindrical containers is also referenced. In addition, the concepts of liquid-induced roll and yaw (side) moment coefficients, by Murphy,[1] are described.

[1] Murphy, C.H., "Angular Motion of a Spinning Projectile with a Viscous Liquid Payload," ARBRL-MR-03194, U.S. Army Ballistic Research Laboratory, Aberdeen Proving Ground, Maryland, August 1982. (AD A118676) Also AIAA Journal of Guidance, Control, and Dynamics, Vol. 6, No. 4, pp.280-286, July-August 1983.

[2] Gerber, N. and Sedney, R. "Moment on a Liquid-Filled Spinning and Nutating Projectile: Solid Body Rotation," ARBRL-TR-02470, U.S. Army Ballistic Research Laboratory, Aberdeen Proving Ground, Maryland, February 1983 (AD A125332).

[3] Murphy, C. H., "Moment Induced by a Liquid Payload During Spin-Up Without a Critical Layer," ARBRL-TR-02581, U.S. Army Ballistic Research Laboratory, Aberdeen Proving Ground, Maryland, August 1984. (AD A145716) Also AIAA Journal of Guidance, Control, and Dynamics, Vol. 8, No. 3, pp.354-359, May-June 1985.

[4] Gerber N., "Liquid Moment on a Filled Coning Cylinder During Spin-Up: Ad Hoc Model," ARBRL-TR-2628, U.S. Army Ballistic Research Laboratory, Aberdeen Proving Ground, Maryland, December 1984. (AD 150280)

[5] D'Amico W. P., "Flight Data on Liquid-Filled Shell for Spin-Up Instabilities," ARBRL-MR-03334, U.S. Army Ballistic Research Laboratory, Aberdeen Proving Ground, Maryland, February 1984. (AD 139136) Also AIAA Paper 83-2143, August 1983.

[6] Nusca M. J., D'Amico W. P., and Beims, W. G., "Pressure Measurements in a Rapidly Rotating and Coning, Highly Viscous Fluid," ARBRL-MR-03325, U.S. Army Ballistic Research Laboratory, Aberdeen Proving Ground, Maryland, November 1983. (AD A136824)

[7] Hepner, D.J., Kendall, T.M., Davis, B.S., and Tenly, W.Y., "Pressure Measurements in a Liquid-Filled Cylinder Using A Three-Degree-Of-Freedom Flight Simulator," ARBRL-MR-3560, U.S. Army Ballistic Research Laboratory, Aberdeen Proving Ground, Maryland, December 1986 (AD A177672). Also, AIAA Paper No. 86-2026, 1986.

[8] Strikwerda, J. C., and Nagel, Y. M., "A Numerical Method for the Incompressible Navier-Stokes Equations in Three-Dimensional Cylindrical Geometry," Journal of Computational Physics, Vol. 78, pp. 64-78, 1988. Also, Strikwerda, J. C., and Nagel, Y. M., "A Numerical Study of Flow in Spinning and Coning Cylinders," CRDC-SP-86007, Proceedings of the 1985 Scientific Conference on Chemical Defense Research, Aberdeen Proving Ground, Maryland, April 1986.

[9] Nusca, M. J., "Computational Fluid Dynamics Methods for Low Reynolds Number Precessing/Spinning Incompressible Flows," ARBRL-MR-03657, U.S. Army Ballistic Research Laboratory, Aberdeen Proving Ground, Maryland, April 1988 (AD A193891).

## 1. Cylindrical Containers.

Strikwerda and co-workers[8] have developed a steady-state, finite-difference, incompressible Navier-Stokes method for fully-filled cylindrical containers. The code employs an implicit, iterative, finite-difference method based on modified line successive-over-relaxation and a pressure update from the gradient of the velocity field. This code (denoted UWISC for University of Wisconsin) employs a non-uniform grid to resolve the velocity and pressure gradients near the cylinder walls, central finite-differences in the radial and axial directions, and pseudo-spectral differencing to represent the azimuthal dependence. Comparison of UWISC with other finite-difference codes, finite-element codes, and analytical methods is reported in Reference 9.

A spatial eigenvalue method has been developed by Hall, Sedney, and Gerber[10] (denoted HSG) for fully-filled cylindrical containers and constant-amplitude coning motion. Murphy et.al.[11] extended this method to partial-fill, fully-filled with central rod, two immiscible liquids, and slow changes to the amplitude of the coning motion. The Navier-Stokes equations are written in an inertial reference frame. They are then reduced to a set of linear partial differential equations based on small angle coning motion, and linear departures from solid body rotation are considered. No slip boundary conditions are imposed at the cylinder walls which makes all flow variables proportional to $e^{i(ft-\theta)}$ where $f$ is the component of the projectile spin along the symmetry axis and $t$ is time. A particular solution was employed which satisfies the axis and lateral wall boundary conditions but not endwall conditions. The eigenvalue problem is obtained using separation of variables from which an infinite sequence of complex eigenvalues is generated. The eigenvalues are determined by an iterative process for which sufficiently accurate initial estimates are required for convergence. The flow variables are expressed as eigenfunction expansions with the coefficients determined by satisfying the endwall boundary conditions. A least squares and collocation method have been used for this purpose. Comparisons of measured liquid moment coefficients with the spatial eigenvalue code (HSG) and UWISC results[9] have shown the consistency of both methods. However, since spatial eigenvalue methods yield results in significantly less computer run time, they are perhaps the preferred scheme for cylindrical containers.

## 2. Non-cylindrical Containers – High Reynolds Number Flow.

A theory for non-cylindrical, axisymmetric, liquid-filled containers has been presented by Wedemeyer.[12] This theory is derived from the linearized, inviscid Navier-Stokes equations, thus $Re = \infty$. Using this theory, the approximate eigen-frequencies of the liquid oscillations can be computed. Liquid moments occur whenever any of the eigen-frequencies fall within a certain bandwidth of the fast yaw (precessional) frequency of the projectile. Liquid-filled, non-cylindrical cavities can be examined where the radius of the

[10] Hall, P., Sedney, R., and Gerber, N., "Fluid Motion in Spinning, Coning Cylinder via Spatial Eigenfunction Expansions," ARBRL-TR-2813, U.S. Army Ballistic Research Laboratory, Aberdeen Proving Ground, Maryland, August 1987.

[11] Murphy, C.H., Bradley, J.W., and Mermagen, W.H., "Liquid Side Moment Exerted by a Spinning, Coning, Highly Viscous Liquid Payload," U.S. Army Ballistic Research Laboratory, Aberdeen Proving Ground, Maryland, report in preparation.

[12] Wedemeyer, E.H., "Dynamics of Liquid Filled Shell: Non-Cylindrical Cavity," BRL Report No. 1326, U.S. Army Ballistic Research Laboratory, Aberdeen Proving Ground, Maryland, August 1966.

cavity is a slowly varying function of the distance along the cavity axis, $|da/dz| \ll 1$. For cylindrical cavities, the inviscid eigen-frequencies are computed exactly and given in Stewartson tables.[13] For small deviations from cylindrical shape, small changes of the eigen-frequencies must be expected. Karpov[14] showed experimentally that rounding the corners of the cylindrical cavity produced very little effect on the range of instability. However, considerable change resulted from modifications such as the conical reduction of one or both ends of the cavity. Wedemeyer's theory agreed favorably with Karpov's data.

## 3. Non-cylindrical Containers – Low Reynolds Number Flow.

Written at the U.S. Army Ballistic Research Laboratory (BRL), the present CFD code is a modified version of UWISC (denoted UWISC/BRL). Like the UWISC code, the UWISC/BRL code uses a finite-difference method for the non-linear, fully viscous Navier-Stokes equations. The computational algorithm is not efficient for flow Reynolds numbers above 300 (see Section IV.2). The contained flowfield and the liquid-induced moments are computed for axisymmetric containers of arbitrary shape. One application is for cylinders with rounded endcaps where $|da/dz| \geq 0$. The endcap is a circular arc where the cap height above the flat endwall, at the axis of the cylinder, is $e/a$. For a hemispherical endcap, $e/a = 1$ (see Figure 1).

## 4. Liquid Roll and Side Moment Coefficients.

Dimensional analysis and linear theories [1,2] indicate that the liquid moment coefficients (roll and yaw or side) will depend upon the following dimensionless parameters:

$$\text{Linear Liquid Moment Coeff.} = F[\text{Re}, c/a, \tau, \dot{K_c}/\dot{\phi}] \tag{1}$$

Given the use of a steady-state CFD code that retains the nonlinear terms, then the liquid moment coefficient will also depend upon the precession angle ($K_c = \sin\alpha_c$). However, the UWISC steady-state code requires $\dot{K_c} = 0$. Hence, this code would yield a dependence as follows:

$$\text{Steady} - \text{State Nonlinear Liquid Moment Coeff.} = F[\text{Re}, c/a, \tau, K_c] \tag{2}$$

The case for low Re should also follow this formulation and will be examined using the dimensionless parameters as guides. It is highly possible that the liquid moment coefficients are linearly related to $\alpha_c$ for $\alpha_c \leq 20$ degrees[9]. If this is the case, then two of the remaining three parameters can be held constant, while the behavior of the liquid moment coefficient upon the third parameter can be explicitly shown.

[13] Stewartson, K., "On The Stability of a Spinning Top Containing Liquid," Journal of Fluid Mechanics, Vol. 5, Pt. 4, 1959.

[14] Karpov, B.G., "Dynamics of Liquid Filled Shell: Resonance in Modified Cylindrical Cavities," BRL Report No. 1332. U.S. Army Ballistic Research Laboratory, Aberdeen Proving Ground, Maryland, August 1966.

Murphy[15] suggested the use of roll and side moment coefficients for small, fixed precession angles, $\alpha_c$, as defined below:

$$\text{Roll Moment} = m_l a^2 \dot{\phi}^2 [C_{\text{LRM}_O} + \tau K_c^2 C_{\text{LRM}}] \tag{3}$$

$$\text{Transverse Moment} = m_l a^2 \dot{\phi}^2 \tau [C_{\text{LSM}} + i C_{\text{LIM}}] K_c e^{i\phi_c} \tag{4}$$

where,

$m_l$      is the mass of liquid in a fully-filled cylindrical container $(2\pi\rho_l a^2 c)$

$a$      is the maximum radius of the container

$\dot{\phi}$      is the spin rate of the container in the inertial frame

$\tau$      is the ratio of coning rate to spin, $\dot{\phi}_c/\dot{\phi}$

$C_{\text{LRM}}$      is the steady-state liquid roll moment coefficient due to coning motion

$C_{\text{LRM}_O}$      is the liquid roll moment coefficient due to transient liquid effects (i.e. spinup)

$C_{\text{LSM}}$      is the liquid side moment coefficient

$C_{\text{LIM}}$      is the liquid in-plane moment coefficient

$K_c$      is $\sin\alpha_c$, where $\alpha_c$ is the precession angle

$\phi_c$      is the phase angle of the coning motion

Further, Reference 15 gives a relationship between the moment coefficients for the linearized, viscous Navier-Stokes equations. Hence, for small precession angles and independent of the Reynolds number,

$$C_{\text{LRM}} = -C_{\text{LSM}} \tag{5}$$

For arbitrary precession angles, Rosenblat[16] has shown that,

$$C_{\text{LRM}} = -C_{\text{LSM}}\tan\alpha_c \tag{6}$$

## III. COMPUTATIONAL APPROACH

In this section the implicit finite-difference method is described. The approach follows that of Strikwerda[8] for a cylindrical container. In certain aspects of the method basic changes were required for a non-cylindrical container (e.g. computational grid, grid stretching, boundary conditions). In particular the numerical code was originally written assuming cylindrical geometry throughout. Certain other aspects of the method are applicable to a non-cylindrical, axisymmetric container (e.g. psuedo-spectral differencing). These differences and similarities in the method are highlighted in the following subsections.

[15] Murphy, C. H., "A Relation Between Liquid Roll Moment and Liquid Side Moment," AIAA Journal of Guidance, Control and Dynamics, Vol. 8, No. 2, pp. 287-288, March-April 1985. Also ARBRL-MR-03347, U.S. Army Ballistic Research Laboratory, Aberdeen Proving Ground, Maryland, April 1984. (AD A140668)

[16] Rosenblat, S., Gooding, A., and Engleman, M. S., "Finite Element Calculations of Viscoelastic Flu' Flow in a Spinning and Nutating Cylinder," CRDEC-CR-87021, U.S. Army Chemical Research, Development and Engineering Center, Aberdeen Proving Ground, Maryland, December 1986.

## 1. Equations of Motion

Consider a fluid-filled container which is spinning about its geometric axis with spinrate $\Omega_s$ and about the coning axis with spinrate $\dot{\phi}_c$ (see Figure 1). The coning axis is fixed in the inertial (Earth-fixed) reference frame. The container axis is inclined to the coning axis by a fixed angle, $\alpha_c$. The fluid velocity $\vec{V}$ and pressure $p$ in the container are governed by the incompressible Navier-Stokes equations for constant viscosity. These equations in an inertial, cartesian coordinate system are given by,

$$\rho \frac{D\vec{V}}{Dt} = -\nabla p + \mu \nabla^2 \vec{V} \tag{7}$$

$$\nabla \cdot \vec{V} = 0 \tag{8}$$

These equations can be transformed to a non-inertial reference frame so that the fluid motion becomes steady and thus time derivatives are zero, $\partial/\partial t = 0$. This reference frame rotates with angular velocity $\dot{\phi}_c$ about the coning axis and was also used by Strikwerda.[8] Reference 8 gives the details of the transformation. In addition, the cylindrical coordinate system is used in which the radial, azimuthal, and axial directions are denoted $r, \phi, z$ with velocity components $u, v, w$. The cylindrical coordinate system is also used in the endcaps where the grid lines are not aligned with the $r, z$ directions.

The equations and variables are non-dimensionalized by the maximum radius of the container ($a$) and with the inertial spinrate ($\dot{\phi} = \Omega_s + \dot{\phi}_c \cos\alpha_c$) and the container radius, as the velocity scale ($a\dot{\phi}$). Thus, the Reynolds number and the precessional frequency are defined as,

$$Re = \frac{a^2 \dot{\phi}}{\nu} \tag{9}$$

$$\tau = \frac{\dot{\phi}_c}{\dot{\phi}} \tag{10}$$

where the kinematic viscosity of the fluid is $\nu = \mu/\rho_l$.

The solid-body rotation is subtracted from the velocity, and the pressure is redefined such that,

$$\vec{V} = \vec{V}_{\text{computed}} + \vec{V}_{\text{solid-body}} + \vec{\tau} \times \vec{r} \tag{11}$$

$$p = p_{\text{computed}} + \frac{r^2}{2} + r^2 \tau \cos\alpha_c + \frac{\tau^2}{2} \left[ (r\cos\phi\cos\alpha_c + z\sin\alpha_c)^2 + r^2\sin^2\alpha_c \right] \tag{12}$$

The resultant equations are given by Strikwerda[8] as,

$$\frac{1}{Re}\Delta(u) - u_{\text{conv}} - u_{\text{corl}} - \frac{\partial p}{\partial r} = 0 \tag{13}$$

$$\frac{1}{Re}\Delta(v) - v_{\text{conv}} - v_{\text{corl}} - \frac{1}{r}\frac{\partial p}{\partial \phi} = 0 \tag{14}$$

$$\frac{1}{Re}\Delta(w) - w_{\text{conv}} - w_{\text{corl}} - \frac{\partial p}{\partial z} = -2\tau\sin\alpha_c r\cos\phi \tag{15}$$

5

$$\frac{1}{r}\frac{\partial(ru)}{\partial r} + \frac{1}{r}\frac{\partial v}{\partial \phi} + \frac{\partial w}{\partial z} = 0 \qquad (16)$$

where,

$$u_{\text{conv}} = u\frac{\partial u}{\partial r} + \frac{v}{r}\frac{\partial u}{\partial \phi} + w\frac{\partial u}{\partial z} + \frac{\partial u}{\partial \phi} - \frac{v^2}{r}$$

$$v_{\text{conv}} = u\frac{\partial v}{\partial r} + \frac{v}{r}\frac{\partial v}{\partial \phi} + w\frac{\partial v}{\partial z} + \frac{\partial v}{\partial \phi} - \frac{uv}{r}$$

$$w_{\text{conv}} = u\frac{\partial w}{\partial r} + \frac{v}{r}\frac{\partial w}{\partial \phi} + w\frac{\partial w}{\partial z} + \frac{\partial w}{\partial \phi}$$

$$u_{\text{corl}} = 2w\tau\sin\alpha_c\sin\phi - 2v(\tau\cos\alpha_c + 1)$$

$$v_{\text{corl}} = 2w\tau\sin\alpha_c\cos\phi + 2u(\tau\cos\alpha_c + 1)$$

$$w_{\text{corl}} = -2\tau\sin\alpha_c(u\sin\phi + v\cos\phi)$$

$$\Delta(u) = \frac{1}{r}\frac{\partial}{\partial r}\left(r\frac{\partial u}{\partial r}\right) + \frac{1}{r^2}\frac{\partial^2 u}{\partial \phi^2} + \frac{\partial^2 u}{\partial z^2} - \frac{2}{r^2}\frac{\partial v}{\partial \phi} - \frac{u}{r^2}$$

$$\Delta(v) = \frac{1}{r}\frac{\partial}{\partial r}\left(r\frac{\partial v}{\partial r}\right) + \frac{1}{r^2}\frac{\partial^2 v}{\partial \phi^2} + \frac{\partial^2 v}{\partial z^2} + \frac{2}{r^2}\frac{\partial u}{\partial \phi} - \frac{v}{r^2}$$

$$\Delta(w) = \frac{1}{r}\frac{\partial}{\partial r}\left(r\frac{\partial w}{\partial r}\right) + \frac{1}{r^2}\frac{\partial^2 w}{\partial \phi^2} + \frac{\partial^2 w}{\partial z^2}$$

## 2. Computational Grid

The equations of motion are solved on a discrete grid that covers the entire flow domain. Figure 2 shows a typical grid for a cylinder of aspect ratio $c/a = 1.486$ with rounded endcaps of height, $e/a = 1$. Only the portion of the container bounded by $0 \le r/a \le 1, \phi = 0°, 0 \le z/a \le (c/a + e/a)$ is displayed in Figure 2. In this example there are 31 grid points in the $r$-direction, 81 grid points in the $z$-direction and 19 grid points in the endcaps (i.e. 5° spacing). The particular grid configuration was chosen for the endcap region to insure that grid cells are four-sided (in the $\phi$ = constant plane) except at the axis, $r/a = 0$. The axis grid line is a boundary, along which boundary conditions are prescribed, and is not part of the computational domain. Thus multiple grid points at this location are inconsequential. Grid stretching is used to insure adequate grid spacing at the walls so that boundary layers and viscous shear stresses are accurately resolved. This is accomplished using the following transformations,[17]

$$r/a = \frac{d\{[(d+1)/(d-1)]^\lambda - 1\}}{1 + [(d+1)/(d-1)]^\lambda} \qquad (17)$$

[17] Nusca, M.J., "Numerical Simulation of Unsteady Incompressible Flow in a Partially-Filled Rotating Cylinder," ARBRL-TR-02915, U.S. Army Ballistic Research Laboratory, Aberdeen Proving Ground, Maryland, June 1988 (AD A196001).

$$z/a = \frac{(c/a)(1 - b + (1 + b)[(b+1)/(b-1)]^{\eta-1})}{1 + [(b+1)/(b-1)]^{\eta-1}} \tag{18}$$

where $\lambda$ and $\eta$ are uniformly spaced coordinates in the $r$ and $z$ directions, respecively. The parameters $d < 1$ and $b < 1$ are chosen to achieve the desired clustering, with very fine boundary spacing for $d \ll 1$ and $b \ll 1$.

## 3. Computational Algorithm

The numerical method used to solve the equations of motion is based on the finite difference scheme of Strikwerda[18] and a psuedo-spectral method. Finite differences are used to approximate derivatives in the radial ($r$) and axial ($z$) directions and the psuedo-spectral method is used to approximate derivatives in the azimuthal direction ($\phi$). Use of the psuedo-spectral method is possible since the flow variables vary in a periodic fashion in the $\phi$ direction. Since the non-cylindrical geometry under consideration in this work is also axisymmetric, the periodicity in $\phi$ is preserved in the endcaps. This results in substantial savings in computer memory and execution time requirements.

Strikwerda[18] has shown that the use of "regularized" finite differences, instead of central difference formula, allows the equations to be solved on a highly stretched grid without loss in accuracy. As examples of the regularized differences, $\partial p/\partial z$ and $\partial w/\partial r$ are approximated by,

$$\frac{\partial p}{\partial z} \simeq \frac{p_{k+1} - p_{k-1}}{2\Delta z} - \frac{p_{k+2} - 3p_{k+1} + 3p_k - p_{k-1}}{6\Delta z} \tag{19}$$

$$\frac{\partial w}{\partial r} \simeq \frac{w_{i+1} - w_{i-1}}{2\Delta r} - \frac{w_{i+1} - 3w_i + 3w_{i-1} - w_{i-2}}{6\Delta r} \tag{20}$$

where $i$ and $k$ represent the radial and axial indicies, respectively, with $i = 1$ to $I$ and $k = 1$ to $K$. Grid spacings are represented by $\Delta r$ and $\Delta z$. Using the psuedo-spectral method, approximations to the pressure derivatives, for example, with respect to the angular variable, $\phi$, are written as[8],

$$\left(\frac{\partial p}{\partial \phi}\right)_{i,j,k} \simeq \sum_{n=0}^{(J/2)'} n a_{i,n,k}\cos n\phi_j - n b_{i,n,k}\sin n\phi_j \tag{21}$$

where $j$ represents the azimuthal indicie with $j = 1$ to $J$. The coefficients are given by,

$$a_{i,n,k} = \frac{2}{J}\sum_{j=0}^{J-1} p_{i,j,k}\sin n\phi_j$$

$$b_{i,n,k} = \frac{2}{J}\sum_{j=0}^{J-1} p_{i,j,k}\cos n\phi_j$$

The boundary conditions on the container walls follow from the no-slip condition for velocity and extrapolation from the interior flow for the pressure.

$$u_{I,j,k} = u_{i,j,1} = u_{i,j,K} = 0$$

[18] Strikwerda, J.C., "Finite Difference Methods for the Stokes and Navier-Stokes Equations," SIAM Journal of Scientific and Statistical Computing, Vol. 5, No. 1, March 1984.

$$v_{I,j,k} = v_{i,j,1} = v_{i,j,K} = 0$$

$$w_{I,j,k} = w_{i,j,1} = w_{i,j,K} = 0$$

$$p_{I,j,k} = 3p_{I-1,j,k} - 3p_{I-2,j,k} + p_{I-3,j,k}$$

$$p_{i,j,1} = 3p_{i,j,2} - 3p_{i,j,3} + p_{i,j,4}$$

$$p_{i,j,K} = 3p_{i,j,K-1} - 3p_{i,j,K-2} + p_{i,j,K-3}$$

The boundary conditions on the container axis ($z$-axis) are obtained using interpolation from neighboring grid points, for example,

$$w_{1,j,k} = \frac{1}{3}\left(\frac{4}{J}\sum_{j=1}^{J} w_{2,j,k} - \frac{1}{J}\sum_{j=1}^{J} w_{3,j,k}\right)$$

$$p_{1,j,k} = \frac{1}{3}\left(\frac{4}{J}\sum_{j=1}^{J} p_{2,j,k} - \frac{1}{J}\sum_{j=1}^{J} p_{3,j,k}\right)$$

Variables at the grid points on the container axis at the interface between the cylinder and the endcaps ($r = 0, z = |c/a|$) are assigned equal values. These values are obtained from interpolation as above.

The system of non-linear equations is solved using a modified line successive-over-relaxation method (LSOR). The method is described by Strikwerda[19] for the case of linear finite difference equations. Because the psuedo-spectral method is used in the azimuthal direction, line relaxation is utilized. In this case each line contains the grid points in the azimuthal direction for each value of the radial and axial coordinates. This approach is unchanged for the non-cylindrical axisymmetric geometry. The coupling between the velocity components and the natural periodicity of the azimuthal coordinate leads to a periodic system of equations. Thus the system of equations that must be solved to determine the velocity updates for each radial and axial grid location is a block tridiagonal periodic linear system. After the velocity has been updated by one pass of the LSOR, the pressure is updated using,

$$p^{m+1} = p^m - \beta\left(\nabla \cdot \vec{V}^{m+1}\right) \tag{22}$$

where $m$ is the iteration index and $\beta$ is a parameter. Thus $\nabla \cdot \vec{V} = 0$ is not solved but rather $\nabla \cdot \vec{V} = \delta$ where $\delta$ is on the order of the truncation error for a second-order scheme.

## 4. Calculation of Liquid-Induced Moments.

Conservation of angular momentum for the steady flow in a control volume V with surface S rotating with constant angular rate $\Omega$ about a fixed axis requires,

$$\vec{M} = \int_S \left(\vec{r} \times \vec{F}\right) dS$$

$$= \int_V \vec{r} \times \left(2\vec{\Omega} \times \vec{V}\right) \rho dV + \int_V \vec{r} \times \left[\vec{\Omega} \times \left(\vec{\Omega} \times \vec{r}\right)\right] \rho dV + \int_S \left(\vec{r} \times \vec{V}\right) \rho \vec{V} \cdot dS \tag{23}$$

[19] Strikwerda, J.C., "An Iterative Method for Solving Finite Difference Approximations to the Stokes Equations," SIAM Journal of Numerical Analysis, Vol. 21, No. 3, June, 1984.

where the velocity $\vec{V}$ is measured relative to the non-inertial reference frame. In this equation, $\vec{M}$ and $\vec{F}$ are the resultant moment on the control volume and the stress acting on the walls of the fully-filled container, respectively. The last term on the right-hand side of the equation vanishes since $\vec{V} \cdot \mathrm{dS} \equiv 0$ on all boundaries. Thus the moment can be calculated using the "surface integral" approach or the "volume integral" approach. The moment can be expressed in terms of the cartesian components, $\vec{M} = (M_x, M_y, M_z)$, which denote the yaw, pitch and roll moments, respectively. The yaw and roll components correspond to the side and roll moment coefficients, $C_{\mathrm{LSM}}$ and $C_{\mathrm{LRM}}$. Using the "volume integral" approach, Herbert[20] and Rosenblat[16] have shown that the non-dimensional yaw and roll moments (non-dimensionalized by $\rho_l a^5 \dot{\phi}_c^2$) for a cylindrical control volume can be expressed as,

$$M_x = \frac{2\cos\alpha_c}{\tau} \int_{-\eta}^{\eta} \int_0^{2\pi} \int_0^{r_{\mathrm{max}}} \left( wr^2\cos\phi \right) dr d\phi dz \tag{24}$$

$$M_z = -M_x \tan\alpha_c \tag{25}$$

thus,

$$C_{\mathrm{LSM}} = \frac{1}{\pi(c/a)\tan\alpha_c} \int_{-\eta}^{\eta} \int_0^{2\pi} \int_0^{r_{\mathrm{max}}} \left( wr^2\cos\phi \right) dr d\phi dz \tag{26}$$

$$C_{\mathrm{LRM}} = -C_{\mathrm{LSM}} \tan\alpha_c \tag{27}$$

where $\eta = c/a$ and $r_{\mathrm{max}} = 1$. Murphy[11] has also derived and utilized the "volume integral" in the spatial-eigenvalue method for highly viscous liquids. For a control volume consisting of a cylinder with rounded endcaps, Equations 26 and 27 are used with $\eta = c/a + e/a$ and $r_{\mathrm{max}} = r_{\mathrm{max}}(z)$.

# IV. RESULTS

In this section the effects of rounded endcaps, versus flat endwalls, on the liquid-induced side moment coefficient, $C_{\mathrm{LSM}}$, is examined for a fully-filled cylindrical container. Results are shown for the original cylinder-only version of the finite-difference code, denoted UWISC, and the Hall-Sedney-Gerber spatial eigenvalue code, denoted HSG, for cylindrical geometries. For non-cylindrical geometries, results from the generalized axisymmetric geometry version of the finite-difference code, denoted UWISC/BRL, are presented.

Moments were computed using both the "surface integral" and the "volume integral" approach (see Section III.4). These methods yielded equivalent numerical results for all cases presented in this report. However, the "volume integral" approach requires less computational effort.

Because the HSG code is formulated assuming a small coning angle, all of the UWISC and UWISC/BRL computations were performed for $\alpha_c = 2°$. All UWISC computations presented in this section were performed using the same grid dimensions with variable grid wall spacing. All HSG computations were performed using 15 to 40 eigenvalues for Re 21.5 to 300. In some cases a cubic spline was used to join discrete data points in the following figures.

---

[20] Herbert, T., "On the Viscous Roll Moment in a Spinning and Nutating Cylinder," CRDC-SP-86007, Proceedings of the 1984 Scientific Conference on Chemical Defense Research, Aberdeen Proving Ground, Maryland, April 1985.

## 1. Variation of $C_{LSM}$ with $e/a$.

Figure 3 shows the variation of $C_{LSM}$ with endcap height, $e/a$, for a cylinder of aspect ratio, $c/a = 1.486$. The height of the endcap is measured at the cylinder axis (see Figure 1). For $e/a = 0$ the container is a cylinder with flat endwalls, and for $e/a = 1$ the endcaps are hemispherical. The same value of $C_{LSM}$ for the cylindrical geometry is produced by the UWISC/BRL and HSG codes. The value of $C_{LSM}$ decreases with increasing endcap height, and reaches a minimum for $e/a = 1$. This suggests that the liquid side moment can be reduced by as much as 20% by rounding the endwalls of a cylinder with aspect ratio $c/a = 1.486$ at $Re = 50$. The value of the coning frequency used in this figure ($\tau = .0469$) is typical of ballistic projectiles with liquid payloads. Since an endcap height of 1 represents the limiting case, all subsequent calculations are for $e/a = 1$.

## 2. Variation of $C_{LSM}$ with Re.

Figure 4 shows the variation of $C_{LSM}$ with Reynolds number for endcap heights of 0 and 1, and a cylinder of aspect ratio of 1.486. For the cylindrical geometry, both the UWISC/BRL and HSG codes show the same variation of liquid side moment with Re, including a maximum, or resonance, at about $Re = 75$. Results using the UWISC/BRL code for the same cylinder with hemispherical endcaps show a resonant condition at about $Re = 50$. In addition, the value of $C_{LSM}$ at resonance is about 22% smaller for the cylinder with rounded endcaps. For $Re = 21.5$ the liquid side moment is actually 12% smaller for the cylinder with flat endwalls. However, for Re greater than the resonance value, the addition of rounded endcaps has reduced the $C_{LSM}$ by as much as 55%.

As noted in a previous study[9] the UWISC code becomes computationally inefficient for for $Re \geq 300$. Figure 5 shows the variation of computer (CRAY-XMP/48) CPU time with Reynolds number. In each case the solution for a particular Re was used as a starting solution for the subsequent Re solution. Since the computer time required increases in an almost linear fashion with Re when scratch starts are used, the restart method results in a substantial savings in computer run time. For $Re \leq 100$, solutions can be achieved in 2 to 4 hours using about 30,000 grid points for the cylindrical geometry, and 7000 additional grid points for the rounded endcaps. These values are considered more than adequate for $c/a = 1.486$. In the previous study[9] with cylindrical containers, computer run times were slightly less than 2 hours for the same value of $c/a$ since a smaller grid was used. The $Re=100$ solution for the cylindrical container required slightly more computer time than the cylinder with rounded endcaps. The data from Figure 4 indicate that the maximum $C_{LSM}$ also occurs at about $Re=100$. This indicates that rounding the cylinder endcaps may promote faster solution convergence. For larger values of Re, the computer run time rapidly increases beyond 5 hours and approaches 12 hours for $Re = 300$. Some reduction in run time ($\leq 5\%$) can be realized by changing the value of $\beta$ in Equation 22 (i.e. a converged solution would require fewer iterations) or relaxing the convergence tolerance. Partially-converged solutions (i.e. using relaxed convergence tolerance) for Reynolds Numbers around 10 can require $\leq 2$ CPU hours using a mini-computer (e.g. VAX 8600) and be used for preliminary design applications. This technique results in severe degradation of the accuracy of $C_{LSM}$ values for Re greater than about 20.

10

## 3. Variation of $C_{LSM}$ with $\tau$.

Figure 6 shows the variation of $C_{LSM}$ with coning frequency for Re = 50, endcap heights of 0 and 1, and a cylinder of aspect ratio of 1.486. For the cylindrical geometry, both the UWISC/BRL and HSG codes show the same variation of liquid side moment with $\tau$, including a resonance at $\tau = .5$. Results using the UWISC/BRL code for the same cylinder with hemispherical endcaps show a resonant condition at $\tau = .65$, with a value of $C_{LSM}$ about 20% larger than the $C_{LSM}$ for a cylinder. For $\tau$ greater than about .35, the liquid side moment is actually 50% smaller for the cylinder with flat endwalls. However, for $\tau$ smaller than the resonance value, the addition of rounded endcaps has reduced the $C_{LSM}$ by as much as 19%.

As noted in a previous study[9] the UWISC code cannot be run for $\tau \geq 1$, whereas the HSG code has been used for coning frequencies greater than the spin frequency. This condition can be resolved by reformulating the UWISC code and dividing the governing equations by $\tau$.

## 4. Variation of $C_{LSM}$ with $c/a$.

Figure 7 shows the variation of $C_{LSM}$ with cylinder aspect ratio for Re = 50, $\tau = .0469$, and endcap heights of 0 and 1. For the cylindrical geometry, both the UWISC/BRL and HSG codes show the same variation of liquid side moment with $c/a$, including a resonance at $c/a = 1.2$. Results using the UWISC/BRL code for the same cylinder with hemispherical endcaps show a resonant condition at $c/a = .6$, at about the same value of $C_{LSM}$. For $c/a$ greater than 1.0 the liquid side moment is up to 19% smaller for the cylinder with rounded endcaps. For $c/a$ greater than 2 the value of $C_{LSM}$ is only 2% smaller for cylinders with rounded endcaps. The value of $C_{LSM}$ approaches 0 as $c/a$ approaches 0 for both the cylinder with flat endwalls and the cylinder with hemispherical endcaps. In the case of the hemispherical endcaps, for $c/a = 0$ the container is a sphere. For a sphere, the integration of pressures over the symmetric interior geometry will not produce a contribution to $C_{LSM}$. Additionally, viscous shear stresses will be zero since, for a sphere, steady rotation and precession is simply rigid body rotation about a different axis.

## 5. Application to Flight Tested Payloads.

Pope[21] reported analysis of flight test data for projectiles with highly viscous liquid payloads (i.e. low Reynolds Number) contained in cylinders with large $c/a$. A particular example was for Re = 45.2, $\tau = .123$, $c/a = 4.23$, and $\alpha_c = 2^o$. Table 1 lists the measured $C_{LSM}$ as well as computed $C_{LSM}$ using the HSG and UWISC/BRL codes. Both HSG and UWISC/BRL show a $C_{LSM}$ value 23% smaller than measured for the cylindrical container. The addition of rounded endcaps slightly increases the moment for $e/a < 1$ and decreases the moment by $\leq 1\%$ for $e/a = 1$. The small change in $C_{LSM}$ for this case is consistent with the results of Figure 7 for large aspect ratio containers. In this case "rounding"

[21] Pope, R.L., "Further Analysis of Yawsonde Data From Some Liquid Payload Projectiles," ARBRL-MR-03329, U.S. Army Ballistic Research Laboratory, Aberdeen Proving Ground, Maryland, December 1983 (AD A137256).

the endcaps does not substantially reduce the liquid moment and would not represent an effective solution for unstable projectile flights.

**Table 1.** Application to Flight Tested Payloads.

| $e/a$ | Datum | $C_{LSM}$ |
|-------|-------|-----------|
| 0 | Flight Data[21] | .0550 |
| 0 | BSG | .0424 |
| 0 | UWISC/BRL | .0420 |
| .50 | UWISC/BRL | .0424 |
| .75 | UWISC/BRL | .0421 |
| 1.0 | UWISC/BRL | .0417 |

# V.  CONCLUSIONS

The three-dimensional, steady, laminar, Navier-Stokes equations are solved using an implicit finite-difference scheme based on successive-over-relaxation. The method of Strikwerda, for fluid-filled cylindrical containers, has been extended to non-cylindrical axisymmetric geometries. The liquid side moment coefficient for a cylinder with rounded endcaps is investigated using this code for Reynolds number, $10 \leq Re \leq 300$. Rounded endcaps can decrease the liquid-induced moment by as much as 40% for some values of the Reynolds number, coning frequency, and cylinder aspect ratio. .

Further modification of the code (e.g. ellipsoidal endcaps, partial-fill, etc.) could be accomplished. However, a computational fluid dynamics code for time-dependent, three-dimensional, incompressible flow in arbitrary geometries has been written by Chakravarthy et.al.[22]. This code is a generalized version of a previous code [23,24] that was used for fully-filled cylindrical containers in steady coning motion and flow Reynolds Numbers as high as 500,000. The new code by Chakravarthy uses the same numerical scheme as the previous code but includes a zonal grid scheme to facilitate grid generation in containers of arbitrary shape. The code requires modification of the boundary conditions, reference frame, and equations of motion in order to compute liquids in precessing/spinning containers. However, this code can be more easily modified than UWISC/BRL for free surface boundary conditions, multiple liquids, time-dependent container motion and other cases of interest.

[22] *Pan, D., and Chakravarthy, S.R., "Unified Formulation for Incompressible Flows," AIAA-89-0122, Proceedings of the 27th AIAA Aerospace Sciences Meeting, Reno, NV, January 9-12, 1989.*

[23] *Kwak, D., and Chakravarthy, S.R., "A Three-Dimensional Incompressible Navier-Stokes Flow Solver Using Primitive Variables," AIAA Journal, Vol. 24, No. 3, March 1986, pp. 390-396.*

[24] *Nusca, M.J., and Cooper, G.R., "Computational Fluid Dynamics Method for Unsteady Incompressible Rotating Flow with Impulsive Coning Motion," CRDEC-SP-89005, Proceedings of the 1988 Scientific Conference on Chemical Defense Research, Aberdeen Proving Ground, Maryland, 1989.*
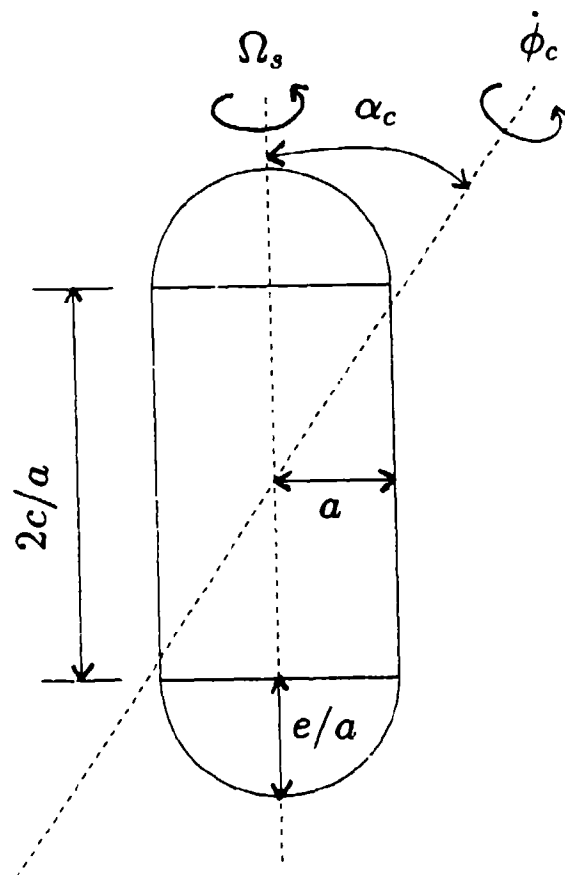
**Figure 1.** Cylinder With Rounded Endcaps – Configuration and Nomenclature (Hemispherical Endcap Shown)
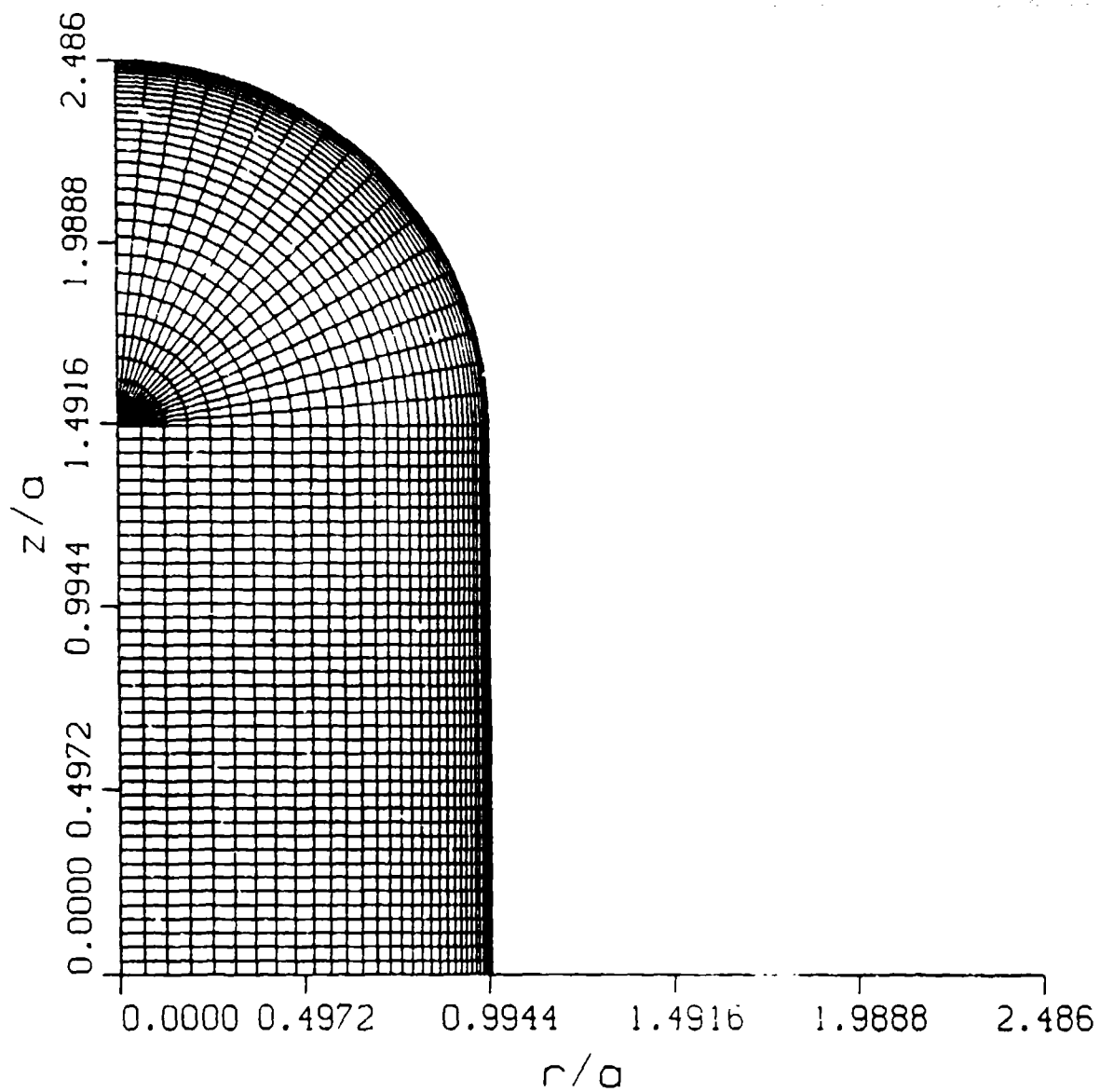
**Figure 2**. Typical Computational Grid (Hemispherical Endcap Shown)

Re = 50 τ = .0469 c/a = 1.486 $\alpha_c$ = 2 deg
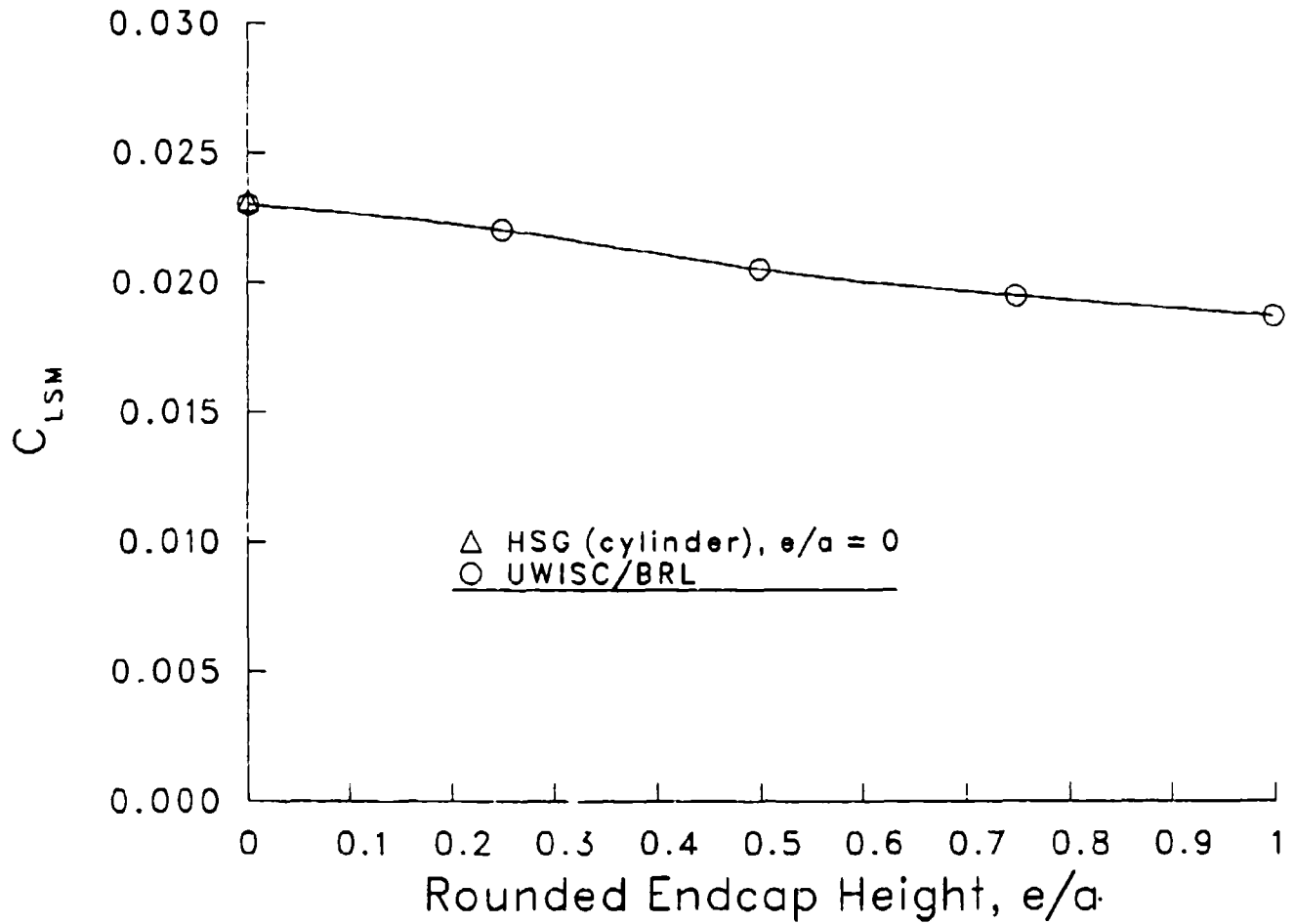


**Figure 3.** Variation of Liquid-Induced Side Moment Coefficient with Rounded Endcap Height; Re = 50, $\tau$ = .0469, $c/a$ = 1.486, $\alpha_c$ = 2°

15

c/a = 1.486   $\tau$ = .0469   $\alpha_c$ = 2 degs.

△ HSG (cylinder), e/a = 0
○ UWISC/BRL (cylinder), e/a = 0
▽ UWISC/BRL, e/a = 1
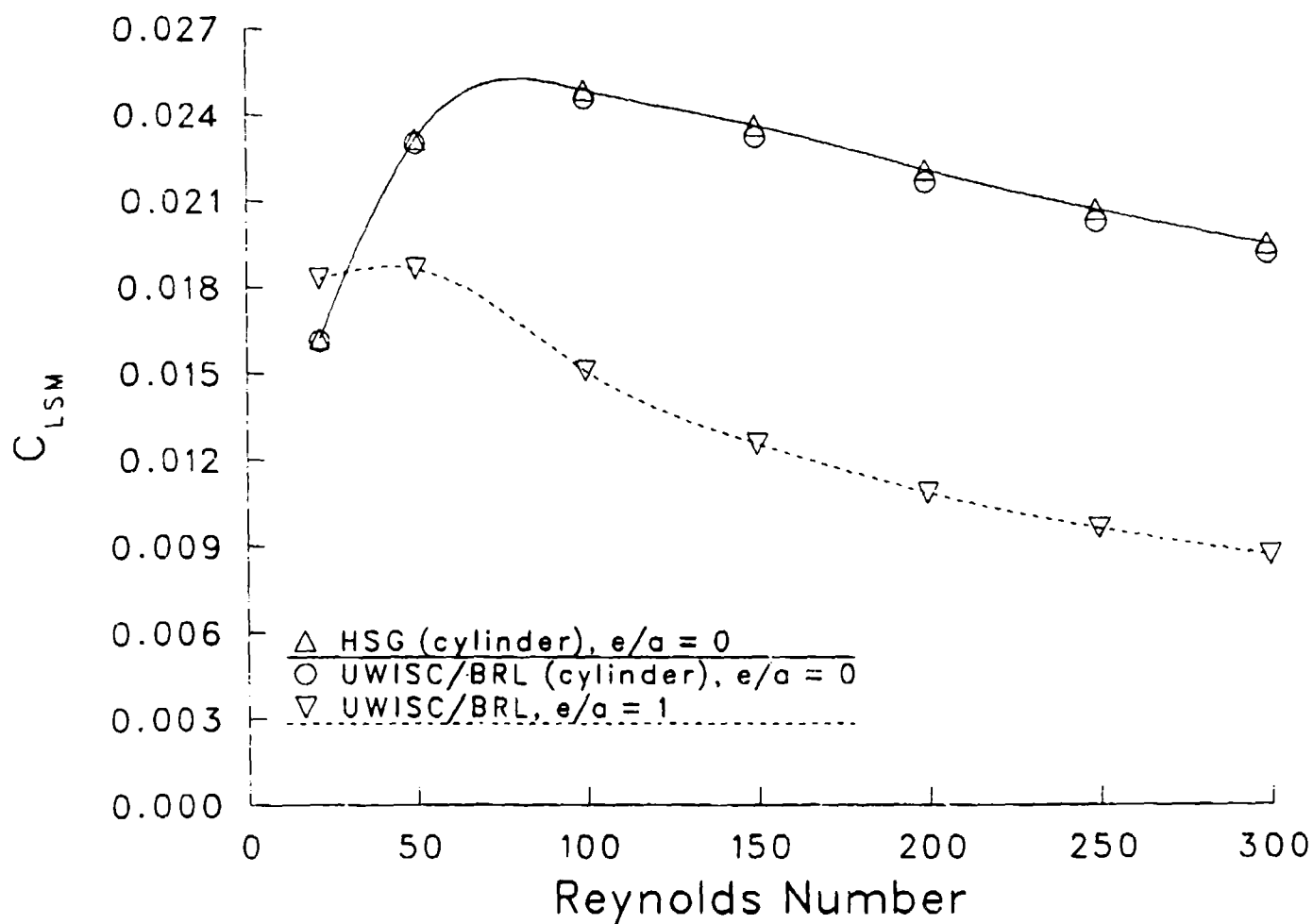
**Figure 4.** Variation of Liquid-Induced Side Moment Coefficient with Reynolds Number; $e/a = 0$ and 1, $\tau = .0469$, $c/a = 1.486$, $\alpha_c = 2°$

16
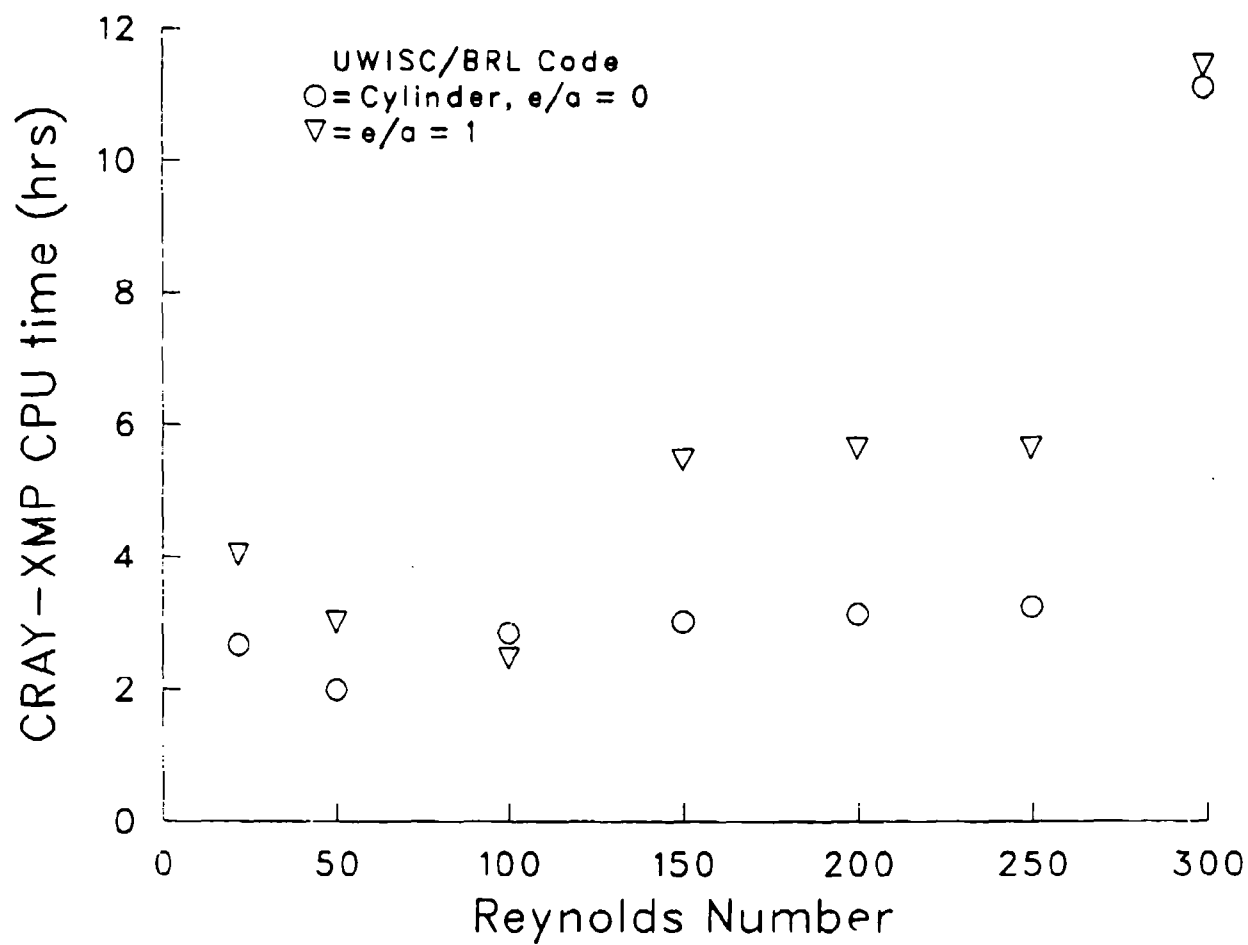
Figure 5. Variation of CRAY-XMP/48 CPU Time with Reynolds Number; $e/a = 0$ and 1, $\tau = .0469$, $c/a = 1.486$, $\alpha_c = 2°$

Re = 50.0   c/a = 1.486   $\alpha_c$ = 2 degs.
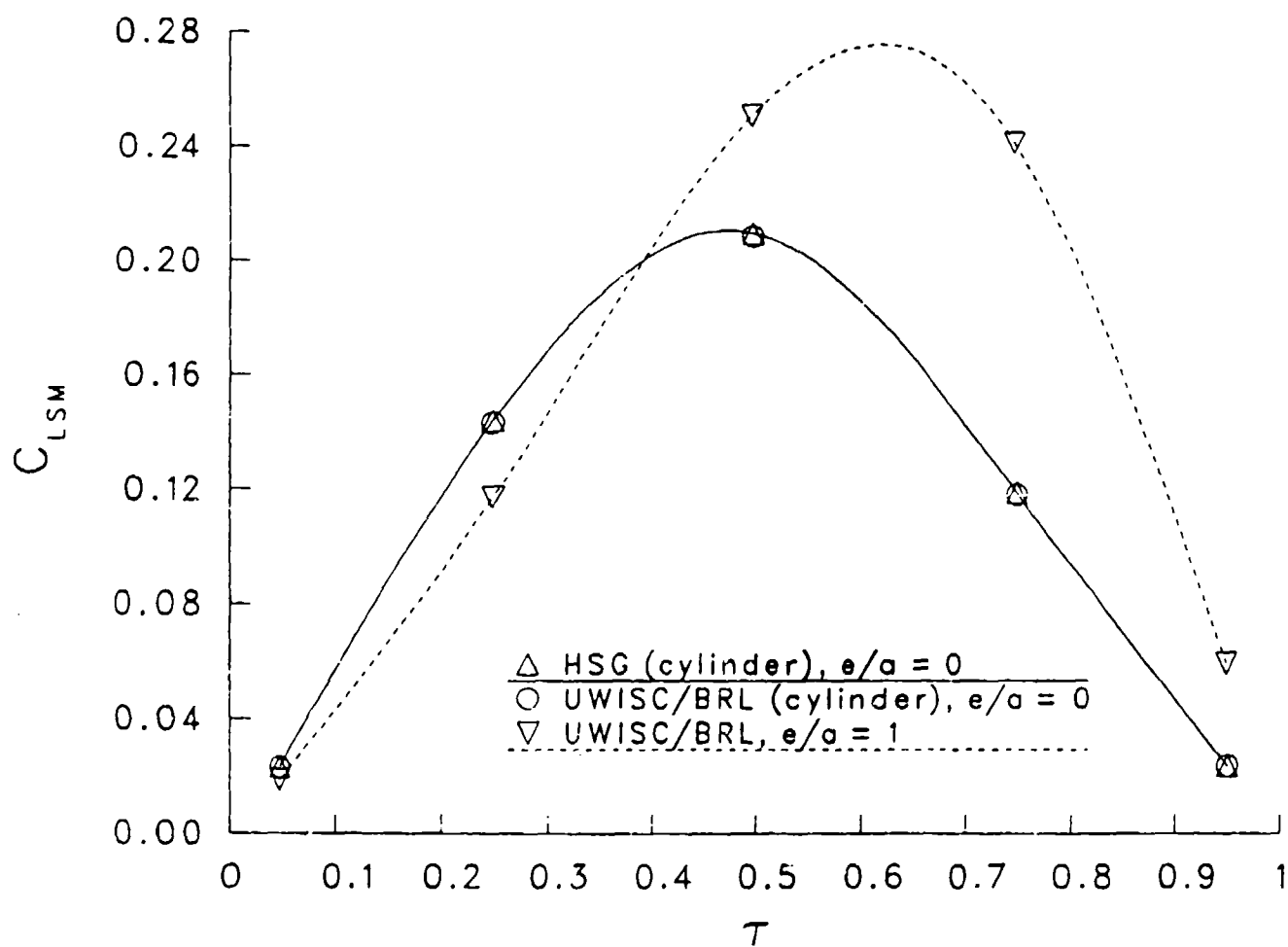


**Figure 6.** Variation of Liquid-Induced Side Moment Coefficient with Coning Frequency; $e/a = 0$ and 1, Re = 50, $c/a = 1.486$, $\alpha_c = 2°$

18
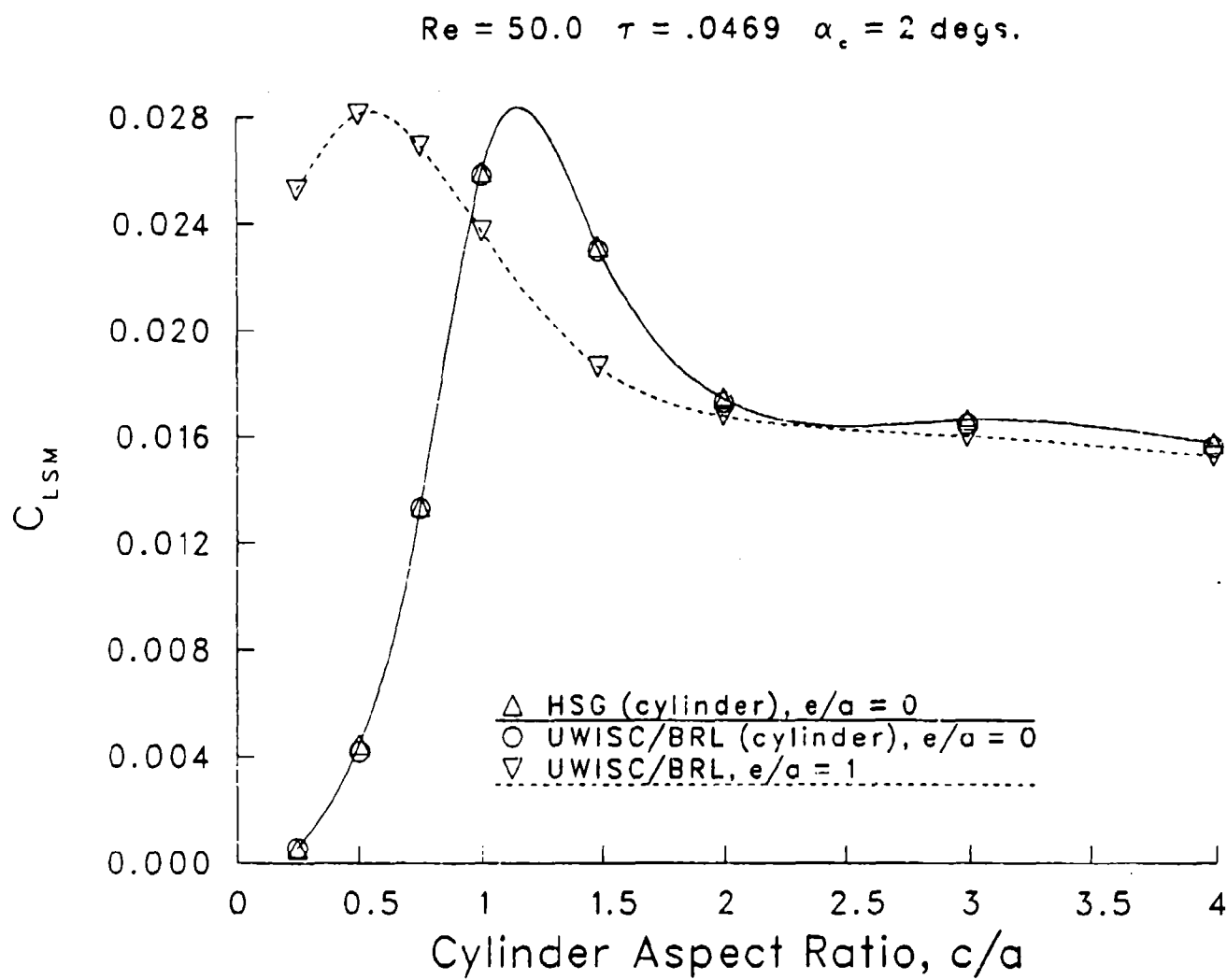
**Figure 7.** Variation of Liquid-Induced Side Moment Coefficient with Cylinder Aspect Ratio; $e/a = 0$ and 1, Re $= 50$, $\tau = .0469$, $\alpha_c = 2°$

# References

1. Murphy, C.H., "Angular Motion of a Spinning Projectile with a Viscous Liquid Payload," ARBRL-MR-03194, U.S. Army Ballistic Research Laboratory, Aberdeen Proving Ground, Maryland, August 1982 (AD A118676). Also, AIAA Journal of Guidance, Control, and Dynamics, Vol. 6, No. 4, pp.280-286, July-August 1983.

2. Gerber, N. and Sedney, R. "Moment on a Liquid-Filled Spinning and Nutating Projectile: Solid Body Rotation," ARBRL-TR-02470, U.S. Army Ballistic Research Laboratory, Aberdeen Proving Ground, Maryland, February 1983 (AD A125332).

3. Murphy, C. H., "Moment Induced by a Liquid Payload During Spin-Up Without a Critical Layer," ARBRL-TR-02581, U.S. Army Ballistic Research Laboratory, Aberdeen Proving Ground, Maryland, August 1984 (AD A145716). Also, AIAA Journal of Guidance, Control, and Dynamics, Vol. 8, No. 3, pp.354-359, May-June 1985.

4. Gerber N., "Liquid Moment on a Filled Coning Cylinder During Spin-Up: Ad Hoc Model," ARBRL-TR-2628, U.S. Army Ballistic Research Laboratory, Aberdeen Proving Ground, Maryland, December 1984 (AD 150280).

5. D'Amico W. P., "Flight Data on Liquid-Filled Shell for Spin-Up Instabilities," ARBRL-MR-03334, U.S. Army Ballistic Research Laboratory, Aberdeen Proving Ground, Maryland, February 1984 (AD 139136). Also, AIAA Paper 83-2143, August 1983.

6. Nusca M. J., D'Amico W. P., and Beims, W. G., "Pressure Measurements in a Rapidly Rotating and Coning, Highly Viscous Fluid," ARBRL-MR-03325, U.S. Army Ballistic Research Laboratory, Aberdeen Proving Ground, Maryland, November 1983 (AD A136824).

7. Hepner, D.J., Kendall, T.M., Davis, B.S., and Tenly, W.Y., "Pressure Measurements in a Liquid-Filled Cylinder Using A Three-Degree-Of-Freedom Flight Simulator," ARBRL-MR-3560, U.S. Army Ballistic Research Laboratory, Aberdeen Proving Ground, Maryland, December 1986. Also, AIAA Paper No. 86-2026, 1986 (AD A177872).

8. Strikwerda, J. C., and Nagel, Y. M., "A Numerical Method for the Incompressible Navier-Stokes Equations in Three-Dimensional Cylindrical Geometry," Journal of Computational Physics, Vol. 78, pp. 64-78, 1988. Also, Strikwerda, J. C., and Nagel, Y. M., "A Numerical Study of Flow in Spinning and Coning Cylinders," CRDC-SP-86007, Proceedings of the 1985 Scientific Conference on Chemical Defense Research, Aberdeen Proving Ground, Maryland, April 1986.

9. Nusca, M. J., "Computational Fluid Dynamics Methods for Low Reynolds Number Precessing/Spinning Incompressible Flows," ARBRL-MR-03657, U.S. Army Ballistic Research Laboratory, Aberdeen Proving Ground Maryland, April 1988 (AD A193891).

10. Hall, P., Sedney, R., and Gerber, N., "Fluid Motion in Spinning, Coning Cylinder via Spatial Eigenfunction Expansions," ARBRL-TR-2813, U.S. Army Ballistic Research Laboratory, Aberdeen Proving Ground, Maryland, August 1987.

11. Murphy, C.H., Bradley, J.W., and Mermagen, W.H., "Liquid Side Moment Exerted by a Spinning, Coning, Highly Viscous Liquid Payload," U.S. Army Ballistic Research Laboratory, Aberdeen Proving Ground, Maryland, report in preparation.

12. Wedemeyer, E.H., "Dynamics of Liquid Filled Shell: Non-Cylindrical Cavity," BRL Report No. 1326, U.S. Army Ballistic Research Laboratory, Aberdeen Proving Ground, Maryland, August 1966.

13. Stewartson, K., "On The Stability of a Spinning Top Containing Liquid," Journal of Fluid Mechanics, Vol. 5, Pt. 4, 1959.

14. Karpov, B.G., "Dynamics of Liquid Filled Shell: Resonance in Modified Cylindrical Cavities," BRL Report No. 1332, U.S. Army Ballistic Research Laboratory, Aberdeen Proving Ground, Maryland, August 1966.

15. Murphy, C. H., "A Relation Between Liquid Roll Moment and Liquid Side Moment," AIAA Journal of Guidance, Control and Dynamics, Vol. 8, No. 2, pp. 287-288, March-April 1985. Also, ARBRL-MR-03347 U.S. Army Ballistic Research Laboratory, Aberdeen Proving Ground, Maryland, April 1984 (AD A140658).

16. Rosenblat, S., Gooding, A., and Engleman, M. S., "Finite Element Calculations of Viscoelastic Fluid Flow in a Spinning and Nutating Cylinder," CRDEC-CR-87021, U.S. Army Chemical Research, Development and Engineering Center, Aberdeen Proving Ground, Maryland, December 1986.

17. Nusca, M.J., "Numerical Simulation of Unsteady Incompressible Flow in a Partially-Filled Rotating Cylinder," ARBRL-TR-02915, U.S. Army Ballistic Research Laboratory, Aberdeen Proving Ground, Maryland, June 1988 (AD A196001).

18. Strikwerda, J.C., "Finite Difference Methods for the Stokes and Navier-Stokes Equations," SIAM Journal of Scientific and Statistical Computing, Vol. 5, No. 1, March 1984.

19. Strikwerda, J.C., "An Iterative Method for Solving Finite Difference Approximations to the Stokes Equations," SIAM Journal of Numerical Analysis, Vol. 21, No. 3, June, 1984.

20. Herbert, T., "On the Viscous Roll Moment in a Spinning and Nutating Cylinder," CRDC-SP-86007, Proceedings of the 1984 Scientific Conference on Chemical Defense Research, Aberdeen Proving Ground, Maryland, April 1985.

21. Pope, R.L., "Further Analysis of Yawsonde Data From Some Liquid Payload Projectiles," ARBRL-MR-03329, U.S. Army Ballistic Research Laboratory, Aberdeen Proving Ground, Maryland, December 1983 (AD A137256).

22. Pan, D., and Chakravarthy, S.R., "Unified Formulation for Incompressible Flows," AIAA-89-0122, Proceedings of the 27th AIAA Aerospace Sciences Meeting, Reno, NV, January 9-12, 1989.

23. Kwak, D., and Chakravarthy, S.R., "A Three-Dimensional Incompressible Navier-Stokes Flow Solver Using Primitive Variables," AIAA Journal, Vol. 24, No. 3, March 1986, pp. 390-396.

24. Nusca, M.J., and Cooper, G.R., "Computational Fluid Dynamics Method for Unsteady Incompressible Rotating Flow with Impulsive Coning Motion," CRDC-SP-89005, Proceedings of the 1988 Scientific Conference on Chemical Defense Research, Aberdeen Proving Ground, Maryland, 1989.

# List of Symbols

| | |
|---|---|
| $a$ | cylinder maximum radius |
| $c$ | cylinder-section half-height |
| $c/a$ | cylinder-section aspect ratio |
| $C_{\mathrm{LRM}}$ | steady-state liquid roll moment coefficient due to coning motion |
| $C_{\mathrm{LRM}_O}$ | liquid roll moment coefficient due to transient liquid spinup |
| $C_{\mathrm{LSM}}$ | liquid side moment coefficient |
| $C_{\mathrm{LIM}}$ | liquid in-plane moment coefficient |
| $e/a$ | ratio of endcap height to maximum cylinder radius |
| $\vec{F}$ | shear stress on the container surface |
| $i,j,k$ | grid indicies for the radial, azimuthal, and axial directions |
| $I,J,K$ | total number of grid points in the radial, azimuthal, and axial directions |
| $K_c$ | $\sin\alpha_c$ |
| $\dot{K}_c$ | yaw growth rate |
| $\vec{M}$ | angular momentum |
| $m_l$ | mass of liquid in a fully-filled cylindrical container $(2\pi\rho_l a^2 c)$ |
| $p$ | static pressure |
| $r$ | radius or radial direction |
| $\vec{r}$ | position vector |
| $\mathrm{Re}$ | Reynolds number, $a^2\dot\phi/\nu$ |
| $S$ | control surface |
| $t$ | time |
| $u,v,w$ | velocity components in the radial, azimuthal, and axial directions |
| $\vec{V}$ | velocity vector |
| $V$ | control volume |
| $z$ | axial direction |

## Greek Symbols

| | |
|---|---|
| $\alpha_c$ | coning or precession angle |
| $\beta$ | parameter, see Equation 22 |
| $\mu$ | molecular viscosity of the liquid |
| $\nu$ | kinematic viscosity of the liquid, $\mu/\rho$ |
| $\rho_l$ | density of the liquid |
| $\tau$ | ratio of coning rate to spin, $\dot\phi_c/\dot\phi$ |
| $\phi$ | azimuthal angle or azimuthal direction |
| $\phi_c$ | phase angle of the coning motion |
| $\dot\phi$ | spin rate of the container in the inertial frame, $\Omega_s + \dot\phi_c\cos\alpha_c$ |
| $\dot\phi_c$ | spin rate of the container about the coning axis |
| $\Omega_s$ | spin rate of the container about the geometric axis |

23

Intentionally left blank.

| No of Copies | Organization | No of Copies | Organization |
|---|---|---|---|
| (Unclass, unlimited) 12 | Administrator | 1 | Commander |
| (Unclass, limited) 2 | Defense Technical Info Center | | US Army Missile Command |
| (Classified) 2 | ATTN: DTIC-DDA | | ATTN: AMSMI-RD-CS-R (DOC) |
| | Cameron Station | | Redstone Arsenal, AL 35898-5010 |
| | Alexandria, VA 22304-6145 | | |

1   HQDA (SARD-TR)
  WASH DC 20310-0001

1   Commander
  US Army Materiel Command
  ATTN: AMCDRA-ST
  5001 Eisenhower Avenue
  Alexandria, VA 22333-0001

1   Commander
  US Army Laboratory Command
  ATTN: AMSLC-DL
  Adelphi, MD 20783-1145

2   Commander
  Armament RD&E Center
  US Army AMCCOM
  ATTN: SMCAR-MSI
  Picatinny Arsenal, NJ 07806-5000

2   Commander
  Armament RD&E Center
  US Army AMCCOM
  ATTN: SMCAR-TDC
  Picatinny Arsenal, NJ 07806-5000

1   Director
  Benet Weapons Laboratory
  Armament RD&E Center
  US Army AMCCOM
  ATTN: SMCAR-LCB-TL
  Watervliet, NY 12189-4050

1   Commander
  US Army Armament, Munitions
  and Chemical Command
  ATTN: SMCAR-ESP-L
  Rock Island, IL 61299-5000

1   Commander
  US Army Aviation Systems Command
  ATTN: AMSAV-DACL
  4300 Goodfellow Blvd.
  St. Louis, MO 63120-1798

1   Director
  US Army Aviation Research
  and Technology Activity
  Ames Research Center
  Moffett Field, CA 94035-1099

1   Commander
  US Army Tank Automotive Command
  ATTN: AMSTA-TSL (Technical Library)
  Warren, MI 48397-5000

1   Director
  US Army TRADOC Analysis Command
  ATTN: ATAA-SL
  White Sands Missile Range, NM 88002-5502

(Class. only) 1   Commandant
  US Army Infantry School
  ATTN: ATSH-CD (Security Mgr.)
  Fort Benning, GA 31905-5660

(Unclass. only) 1   Commandant
  US Army Infantry School
  ATTN: ATSH-CD-CSO-OR
  Fort Benning, GA 31905-5660

(Class. only) 1   The Rand Corporation
  P.O. Box 2138
  Santa Monica, CA 90401-2138

1   Air Force Armament Laboratory
  ATTN: AFATL/DLODL
  Eglin AFB, FL 32542-5000

Aberdeen Proving Ground
Dir, USAMSAA
    ATTN: AMXSY-D
            AMXSY-MP, H. Cohen
Cdr, USATECOM
    ATTN: AMSTE-TO-F
Cdr, CRDEC, AMCCOM
    ATTN: SMCCR-RSP-A
            SMCCR-MU
            SMCCR-MSI
Dir, VLAMO
    ATTN: AMSLC-VL-D

| No. of Copies | Organization | No. of Copies | Organization |
|---|---|---|---|
| 2 | Director<br>Sandia National Laboratories<br>ATTN: Dr. W. Oberkampf<br>Dr. W.P. Wolfe<br>Division 1636<br>Albuquerque, NM 87185 | 1 | North Carolina State University<br>Mechanical and Aerospace<br>Engineering Department<br>ATTN: F.F. DeJarnette<br>Raleigh, NC 27607 |
| 1 | Director<br>National Aeronautics and<br>Space Administration<br>Ames Research Center<br>ATTN: Dr. J. Steger<br>Moffett Field, CA 94035 | 1 | Northwestern University<br>Dept. of Engineering Science<br>and Applied Mathematics<br>ATTN: Dr. S.H. Davis<br>Evanston, IL 60201 |
| 1 | Aerospace Corporation<br>Aero-Engineering Subdivision<br>ATTN: Walter F. Reddall<br>El Segundo, CA 90245 | 1 | Ohio State University<br>Dept. of Mechanical Engineering<br>ATTN: Dr. T. Herbert<br>Columbus, OH 43221 |
| 1 | Calspan Corporation<br>ATTN: W. Rae<br>P.O. Box 400<br>Buffalo, NY 14225 | 1 | Rensselaer Polytechnic Institute<br>Department of Math Sciences<br>Troy, NY 12181 |
| 1 | Hughes Aircraft<br>ATTN: Dr. John McIntyre<br>Mail Code S41/B323<br>P.O. Box 92919<br>Los Angeles, CA 90009 | 1 | University of Colorado<br>Department of Astro-Geophysics<br>ATTN: E.R. Benton<br>Boulder, CO 80302 |
| | | 1 | University of Maryland<br>ATTN: J.D. Anderson<br>College Park, MD 20740 |
| 1 | Rockwell International<br>Science Center<br>ATTN: Dr. S. Chakravarthy<br>1049 Camino Dos Rios<br>P.O. Box 1085<br>Thousand Oaks, CA 91360 | 1 | University of Maryland<br>Baltimore County<br>Department of Mathematics<br>ATTN: Dr. Y.M. Lynn<br>5401 Wilkens Avenue<br>Baltimore, MD 21228 |
| 1 | Arizona State University<br>Department of Mechanical and<br>Energy Systems Engineering<br>ATTN: G.P. Neitzel<br>Tempe, AZ 85281 | 2 | Univ. of Southern California<br>Dept. of Aerospace Engineering<br>ATTN: T. Maxworthy<br>P. Weidman<br>Los Angeles, CA 90007 |
| 1 | Illinois Institute of Technology<br>ATTN: Mr. Simon Rosenblat<br>3300 South Federal<br>Chicago, IL 60616 | 1 | University of Wisconsin-Madison<br>Center for Mathematical Sciences<br>ATTN: Dr. John Strikwerda<br>610 Walnut Street<br>Madison, WI 53706 |
| 1 | Massachusetts Institute of<br>Technology<br>ATTN: H. Greenspan<br>77 Massachusetts Avenue<br>Cambridge, MA 02139 | 1 | VPI and State University<br>Dept. of Aerospace Engineering<br>ATTN: Tech Library<br>Blacksburg, VA 24061 |

No. of
Copies          Organization

1     Mr. Harold Vaughn
      7709 Gladden N.E.
      Albuquerque, NM  87110


Aberdeen Proving Ground

      Director, USAMSAA
        ATTN:  AMXSY-RA, R. Scungio

      Commander, USATECOM
        ATTN:  AMSTE-TE-F, W. Vomocil
               AMCPM-SMK-M, J. Callahan
               PM-SMOKE, Bldg. 324

      Commander, CRDEC, AMCCOM
        ATTN:  SMCCR-MU,
               W. Dee
               C. Hughes
               F. Dagostin
               D. Bromley
               C. Jeffers
               L. Shaft
        ATTN: SMCCR-RSP-A, M. Miller

INTENTIONALLY LEFT BLANK.